HHS Public Access

Author manuscript

Cancer Res. Author manuscript; available in PMC 2021 September 02.

Published in final edited form as:

Cancer Res. 2020 September 01; 80(17): 3568–3579. doi:10.1158/0008-5472.CAN-19-3984.

Cancer-associated point mutations in the *DLC1* tumor suppressor and other Rho-GAPs occur frequently and are associated with decreased function

Dunui Wang[*], **Xiaolan Qian**[*], **Beatriz Sanchez-Solana**[*], **Brajendra K. Tripathi**, **Marian E. Durkin**, **Douglas R. Lowy**

Laboratory of Cellular Oncology, Center for Cancer Research, National Cancer Institute, National Institutes of Health Bethesda, Marylan

Abstract

In advanced cancer, the RHOA GTPase is often active together with reduced expression of genes encoding Rho-specific GTPase-accelerating proteins (Rho-GAP), which negatively regulate RHOA and related GTPases. Here we used the TCGA dataset to examine 12 tumor types (including colon, breast, prostate, pancreas, lung adenocarcinoma and squamous cell carcinoma) for the frequency of codon mutations of 10 Rho-GAP and experimentally tested biochemical and biological consequences for cancer-associated mutants that arose in the DLC1 tumor suppressor gene. DLC1 was the Rho-GAP gene mutated most frequently, with 5–8% of tumors in five of the tumor types evaluated having DLC1 missense mutations. Furthermore, 20–26% of the tumors in four of these five tumor types harbored missense mutations in at least one of the 10 Rho-GAP. Experimental analysis of the DLC1 mutants indicated seven of nine mutants whose lesions were located in the Rho-GAP domain were deficient for Rho-GAP activity and for suppressing cell migration and anchorage-independent growth. Analysis of a DLC1 linker region mutant and a START domain mutant showed each was deficient for suppressing migration and growth in agar, but their Rho-GAP activity was similar to that of wild type DLC1. Compared with the wild type, the linker region mutant bound 14-3-3 proteins less efficiently, while the START domain mutant displayed reduced binding to Caveolin-1. Thus, mutation of Rho-GAP genes occurs frequently in some cancer types and the majority of cancer-associated DLC1 mutants evaluated were deficient biologically, with various mechanisms contributing to their reduced activity.

Corresponding Author: Douglas R. Lowy, National Cancer Institue, National Institute of Health, Building 37, Room 4106, Bethesda, MD 20892. Phone: 240-781-4100; lowyd@mail.nih.gov.

Authors' Contributions

Conception and design:D. Wang, X. Qian, B. Sanchez-Solana, D.R. Lowy

Development of methodology: D. Wang, X. Qian, B. Sanchez-Solana, B.K. Tripathi, D.R. Lowy

Acquisition of data (provided animals, acquired and managed patients, provided facilities, etc.): D. Wang, X. Qian, B. Sanchez-Solana, D.R. Lowy

Analysis and interpretation of data (e.g., statistical analysis, biostatistics, computational analysis):D. Wang, X. Qian, B. Sanchez-Solana, B.K. Tripathi, D.R. Lowy

Writing, review, and/or revision of the manuscript:D. Wang, X. Qian, B. Sanchez-Solana, B.K. Tripathi, M.E. Durkin, D.R. Lowy

Administrative, technical, or material support (i.e., reporting or organizing data, constructing databases):D. Wang, X. Qian, B. Sanchez-Solana, D.R. Lowy

Study supervision: D.R. Lowy

[*]These authors contributed equally to this work

Conflict of Interest Statement: The authors declare no potential conflict of interest.

Introduction

The RHOA GTPase, like most members of the superfamily of small GTPases, cycles between an active GTP-bound form and an inactive GDP-bound form, a process that normally is tightly controlled but is frequently dysregulated during cancer progression (1,2). While the Ras GTPases are often constitutively activated by point mutation in human cancers, RHOA mutations were rarely detected until the advent of new sequencing technologies (3). RHOA mutations are common in certain types of lymphoma (3) and in gastric cancer, especially its diffuse form, where RHOA mutations were found in 25% of these cancers in one study (4). In most other cancer types, increased Rho-GTP levels may be associated with upregulation of Rho-specific guanine nucleotide exchange factors (Rho GEFs), which catalyze exchange of inactive GDP-bound Rho for active GTP-bound Rho, or downregulation of Rho-specific GTPase-accelerating proteins (Rho GAPs), which catalyze hydrolysis of Rho-GTP to Rho-GDP (5,6).

We have been studying the three genes of the *DLC* (Deleted in Liver Cancer) family -- *DLC1(ARHGAP7*, *STARD12*, and *p122-RhoGAP), DLC2 (STARD13)* and *DLC3 (STARD8)* -- which encode Rho-GAP proteins that negatively regulate RHOA, RHOB, and RHOC, localize to focal adhesions in cultured cells, and are down-regulated in a variety of cancers (7,8). Comparative expression of the three genes, which was enabled by The Cancer Genome Atlas (TCGA), indicated that *DLC1* mRNA is expressed at higher levels than *DLC2* and *DLC3* in most normal tissues, and that *DLC1* expression in several cancer types is reduced to a greater degree than *DLC2* and *DLC3* (9).

Thus far, the main mechanisms evaluated for the downregulation of *DLC1–3* expression in tumors have been gene deletion and promoter DNA methylation, although other genetic and epigenetic changes may also contribute to their decreased expression (10). Point mutation of the *DLC* genes in cancer has been examined to a limited degree. Analysis of *DLC1* in gastric cancer cases from Korea and from TCGA by Park et al. determined it was mutated in almost 10% of the tumors (11). However, given the unusually high rate of RHOA mutation in gastric cancer, the mutation frequency of *DLC1* in this cancer might also be higher than in other cancer types. Experimental analysis by Park et al. of four *DLC1* mutants associated with gastric cancer indicated that their growth inhibitory activity was attenuated, relative to wild type *DLC1*, in three of the mutants, which the authors attributed to a reduced half-life of the mutant DLC1 proteins. In an earlier report, several mutations were identified in the “focal adhesion targeting” (FAT) region (amino acids 201–500) of DLC1 in prostate and colon cancer (12). Two of the mutants (T301K and S308I), although they were located outside the Rho-GAP domain of DLC1, had lower Rho-GAP activity and reduced tumor suppressor activity, as determined by a monolayer colony formation assay. Subsequently, Ravi et al reported that DLC1 GAP activity was regulated by EGF-induced phosphorylation and dephosphorylation of T301 and S308, which must be an indirect result of EGFR activation, as the EGF receptor phosphorylates tyrosines (13).

Given this background, it was of interest to determine the mutation frequency of the three *DLC* genes in a range of tumor types, and to experimentally examine the biochemical and biological properties of several cancer-associated missense mutants. In addition, we

have extended the bioinformatic analysis of cancer-associated mutations to several other established or probable Rho-GAPs. The bioinformatic results indicate that more than 20% of several cancer types harbor at least one missense mutation in a Rho-GAP gene, and that *DLC1* is the Rho-GAP gene with highest frequency of missense mutations in most of the evaluated cancer types. Our experimental analysis of *DLC1* mutants with lesions in different parts of the gene indicate that the majority of the mutants tested have an attenuated tumor suppressor activity that can be detected in vitro, and that several biochemical mechanisms can account for the attenuated phenotype of the mutants.

Materials and methods

Bioinformatics and data analysis

The data for the current study are from two sources: TCGA harmonized mutation data from NCI Genomic Data Commons (GDC) Data Portal and the COSMIC database (Catalogue Of Somatic Mutations In Cancer dataset [Cosmic v74, 2015])(14).

Twelve tumor mutation (open-acess) tab-delimited text maf files from the GDC data portal were selected and downloaded (TCGA.*.mutect.*somatic.maf) for data analysis (https://portal.gdc.cancer.gov/repository). A data file from these maf files was generated to import into mysql table (mysql community server 8.0.17). The mutation status of various cancer types was retrieved using the mysql query command. The data file is available upon request. Variant Allele Frequency (VAF) of the individual mutations of TCGA datasets was obtained from cBioPortal website (https://www.cbioportal.org/).

Pearson's correlation coefficient was used to calculate the correlation between the total number of mutations and the number of *DLC1* mutations of 12 tumor types. The total number of mutations per tumor vs. *DLC1* and other Rho-GAP gene mutations in TCGA was determined and analyzed using the GDC data portal derived mysql table. The queried mutation and VAF data were plotted using the ggplot2 package (Violin plot, Supplementary Figure S1), the trackViewer Bioconductor package (Lolliplot, Supplementary Figure S2), and statistical computing and graphics software R (version 3.5.2). Graphic presentation for the patients with *DLC1* mutations and wild type was performed using GraphPad Software Prism software (version 7.0e). For statistical analysis, the Mann-Whitney U test was used and $p < 0.05$ was considered statistically significant.

Generation of cancer-associated missense mutations in *DLC1* cDNA and other constructs

Two templates were used to construct the missense mutants: pEGFP-DLC1, which encodes the full-length *DLC1* variant 2 cDNA fused into the pEGFP-C1vector (15), and pEGFP-GAP, which encodes the Rho-GAP domain of *DLC1* codons 609–878 (16). The primers used to construct the various mutants are listed in Supplementary Table S1. Eighteen cycles of PCR were performed using a site-directed mutagenesis kit (Agilent Technologies) according to the instructions supplied by the manufacturer. All resulting mutations in the *DLC1* plasmids were confirmed by DNA sequencing.

GFP-DLC1 929–957 Del, and GST-tagged human Caveolin-1 (GST-Caveolin-1) plasmids were described previously (17). GST-tagged human 14-3-3 beta, eta, and theta were cloned

by PCR amplification with primers listed in Supplementary Table S1, and subcloned into the pEBG vector through Bam HI-NotI sites.

RT- PCR for detecting endogenous *DLC1* expression

RNA was isolated from the cell lines using TRIzol reagent (Invitrogen), according to the manufacturer's protocol. RNA was reverse transcribed into cDNA using random primers and other reagents from the Invitrogen ThermoScript RT-PCR system kit. The human *DLC1* transcript was detected with forward (5'-CACAGGACAACCGTTGCCTCAG) and reverse (5'-CTCTTCAGGGTGTTGAGATGGA) primers that amplify a 465 bp product (nt 2267–2731 of NM_006094). PCR was performed using Taq DNA polymerase (New England Biolabs), with an initial denaturation of 94° for 3 minutes, followed by 35 cycles of 40 sec at 94°, 40 sec at 55°, 1 min at 72°, and a final extension of 4 min at 72°. As a control, amplifications were performed with human GAPDH forward (5'-GACATCAAGAAGGTGGTGAAGC) and reverse (5'-GATGGTACATGACAAGGTGCGG) primers, which yield a 417 bp product (nt 845–1261 of NM_002046). PCR products were analyzed by agarose gel electrophoresis and ethidium bromide staining.

Cell culture, transfections, and generation of stable cell lines

HEK 293T and human colon cancer SW620 cells were grown in DMEM supplemented with 10% FBS. Human colon cancer HCT 116 and HT-29 cells were grown in Mc Coy's media supplemented with 10% FBS. Human NSCLC lines (H1299 and H1703), human breast cancer cell line MCF-7, and human colon cancer COLO 205 were grown in RPMI supplemented with 10% FBS. Human colon cancer RKO cells were grown in EMEM media supplemented with 10% FBS. All cells were maintained in a humidified atmosphere containing 5% CO_2. All cell lines were obtained from ATCC and confirmed as mycoplasma-negative prior to their use in assays at an early passage (between 10–20).

The Lipofectamine 3000 (Invitrogen) system was used for all transfections, following the manufacturer's protocol. For the generation of stable clones, transfected SW620 cells were cultured for several weeks after G418 (0.8mg/ml) selection. The selected stable clones were validated for GFP or GFP-DLC1 expression by Western blot. The stable clones expressing equivalent transfected wild type or mutant GFP-DLC1 were used for Rhotekin or Pak-1 pull-down assays, as well as for anchorage-independent growth assays.

Transwell migration and anchorage-independent growth assays

The transwell cell migration assay was performed using 6.5 mm diameter Falcon cell culture inserts (8 μM pore size, ThermoFisher) precoated with 0.01% gelatin, in 24 well cell culture plates as described (18). The collected lysates from stained migrated cells were quantified in a spectrophotometer using OD_{590nm}. For soft agar assay, 1×10^5 of G418-resistant stable SW620 clones were mixed with complete media containing 0.4% of ultrapure agar (Invitrogen) and placed over 0.6% basal agar in 6cm dishes in triplicate. Cells were fed with fresh media weekly and grown for 3 weeks, and colonies were stained, photographed microscopically and quantified by a colony counter.

Rhotekin-RBD and Pak1-RBD pull-down assay and immunoblotting

Cells were lysed with Mg^{++} lysis buffer (EMD Millipore) and the total proteins were estimated by BCA assay (Thermo Scientific; (19)). Equal amounts of protein from cell extracts were used for pull-downs with Rhotekin-RBD for RhoA-GTP or Pak1-RBD for CDC42-GTP followed, respectively, by immunoblotting with anti-Rho or anti-Cdc42 antibody according to the manufacturer's instructions (EMD Millipore). The transfected GFP-DLC1 protein or downstream Rho-signaling proteins were analyzed by immunoblotting with anti-GFP (Abcam), p-Cofilin Ser3 or Cofilin (EMD Millipore) antibodies followed by secondary anti-IgG conjugated with HRP (1:10,000, GSS). The signals bound to the membranes were detected by ECL or ECL plus kit (Thermo Scientific).

In vivo GST pull down assays

For GST pull-down assays, HEK 293T cells were co-transfected with plasmids expressing GST or GST fusion proteins together with GFP or GFP-DLC1 constructs. Forty-eight hours after transfection, cells were lysed with 1X RIPA buffer (EMD Millipore) (0.05M Tris-HCl pH 7.4, 0.15mM NaCl, 0.25% deoxycholic acid, 1% NP-40, 1mM EDTA) containing protease and phosphatase inhibitors. Supernatants were collected after centrifugation at 14000 rpm for 10 min at 4° C, and protein was quantified with a BCA kit (Thermo Scientific) following manufacturer's instructions. One and one-half milligrams of protein from each cell extract were used for pull-down assays by adding 30 μl of glutathione Shepharose-4B slurry (GE Healthcare) and rotating 4 hours at 4° C. Pellets were extensively washed for 3–4 times with 1X RIPA buffer and incubated with 40 μl loading buffer. After separating protein samples by SDS-PAGE, immunoblotting was used to detect protein signals with mouse anti-GST (Santa Cruz Biotechnology) or mouse anti-GFP (Covance) antibodies. Horseradish peroxidase-conjugated anti-mouse IgG (GE Healthcare) was used as the secondary antibody. Immunocomplexes were visualized with an ECL kit (Amersham).

Immunofluorescence staining and confocal microscopy

Transfected cells were fixed with 4% paraformaldehyde for 20 min, permeabilized with 0.25% Triton X-100 in PBS for 5 min, and blocked with 3% BSA for 2 hr. The cells were incubated with a 1:500 dilution (in PBS) of theGFP mouse (abcam)and Vinculin primary rabbit (Sigma-Aldrich) antibodies at 4°C overnight. After thorough wash with PBS, the cells were incubated with 1:250 Alexa-conjugated appropriate secondary antibodies for 1 hour. To visualize nuclei, cells were incubated with DAPI (1:2,500) for 1 hour. After staining, cells were thoroughly washed with PBS and mounted with gel mounting solution (Biomeda Corporation). Confocal microscopy of fluorescent-labeled cells was performed using a microscope (LSM 780; Carl Zeiss) with an excitation wavelength of 488 nm to detect transfected GFP fusion proteins. Focal adhesions (Vinculin) were viewed with an excitation wavelength of 568 nm (Alexa Fluor 568). Images were made at RT using photomultiplier tubes with a Plan-Apochromat 63X/1.4 NA oil differential interference contrast objective lens.

Results

Cancer-associated *DLC1* mutations occur frequently in several cancer types

We used the TCGA database to evaluate 12 types of solid tumors for mutations of *DLC1, DLC2, DLC3,* and *RHOA* (Table 1A and B). The 12 cancer types were uterine, melanoma, colon, stomach, rectum, lung adenocarcinoma (lung AD), lung squamous cell (lung SC), esophagus, pancreas, liver, breast, and prostate. Although colon and rectal cancer are often grouped together, they are presented separately here because their mutation frequency was somewhat divergent. In each table, the tumor types are arranged in descending order, from top to bottom, according to the mean number of mutations of any kind per case that affected codons in the tumor type (see the legend to Table 1A for the types of mutations that have been included). The average total number of mutations per tumor type varied more than 20-fold, from 955 for uterine cancer to 40 for prostate cancer. The percentage of tumors with codon mutations of any type (see legend to Table 1A for definition of what these mutations include) for *DLC1–3* and *RHOA* are shown in Table 1A, while the subset of missense mutations for these genes are in Table 1B. For *DLC1–3*, missense mutations accounted for at least 75% of the mutations for most tumor types (compare data in Table 1A and B for each tumor type). For *RHOA*, 80% of the mutations were missense. The data in Table 1A and B confirm that stomach cancer has the highest percentage of mutant *RHOA* and that 7.09% of the stomach cancers have *DLC1* mutations of any kind; 84% of them were missense mutations. The missense *RHOA* mutation rate was 4.58% for stomach cancer (all 20 of the mutations were missense), while it was lower than 2% for the other tumor types.

In contrast to *RHOA*, several tumor types had *DLC1* mutation rates that were similar to or even higher than those in stomach cancer. These included uterine (9.06% for all mutation types and 7.74% for missense mutations), colon (8.52% for all types and 7.02% for missense), lung SC (7.52% for all types and 6.91% for missense), and melanoma (6.85% for all types and 5.57% for missense). In general, the *DLC1* rate of all codon mutations correlated with the average total number of all codon mutations for the tumor type (Figure 1A; r=0.79). However, lung SC was an outlier, as its *DLC1* mutation rate was third highest, while its total average mutation rate was seventh highest, perhaps suggesting that *DLC1* may be even more critical in lung SC than in the other tumor types.

To infer whether these mutations were heterozygous or homozygous, the *DLC1* mutant allele frequency within each tumor was determined for the 10 tumor types with the largest number of *DLC1* missense mutations (colon and rectal tumor mutations were analyzed together). Pancreas and prostate tumors, which had the fewest mutant *DLC1* alleles (Table 1), were not analyzed. The data indicated that most mutations in the various tumor types were heterozygous, although some appeared to be homozygous (Supplementary Figure S1A). We compared this finding with mutations of *NF1*, a more widely studied tumor suppressor gene that encodes a GAP that negatively regulates the Ras proteins, as *NF1* mutations are usually considered biologically relevant (20). Using the same database to perform the analogous analysis for *NF1* mutations, the results indicated that the mutant allele frequency for *NF1* was similar to that of *DLC1* (Supplementary Figure S1B).

The mutation rates for *DLC2* and *DLC3* were lower than for *DLC1* for almost all tumor types. The one exception was the missense rate for *DLC2* in melanoma, which was similar to that of *DLC1* (5.78% for *DLC2* vs. 5.57% for *DLC1*). Most tumors with a mutation of any *DLC* gene had only one *DLC* gene mutation per tumor, although more than one *DLC* gene was mutated in a few tumors. For five tumor types – uterine, melanoma, colon, stomach, and lung SC - at least 10% of the tumors had a missense mutation in one or more *DLC* gene (column “DLC total” in Table 1B). Another three types - rectum, lung AD, and esophagus - had somewhat lower total DLC missense mutation rates (6–8%), while the rates for pancreas, liver, breast, and prostate were much lower (2% or fewer).

When the mean total number of mutations were compared with the median number for a given tumor type, the ratio was 3:1 or lower for most tumor types. Uterine cancer was the most exceptional, with a ratio higher than 10:1, implying that some of the tumors had very high overall mutation rates. Colon cancer, with a ratio of 3.8:1, was the other tumor type with a ratio higher than 3:1. A subset of both of these tumor types are known to have high levels of micro-satellite instability (MSI-high), which is frequently associated with DNA repair defects and a comparatively large number of mutations (21–23). It therefore seemed possible that *DLC* mutations would be more likely to occur in those tumors that had a larger total number of mutations. Consistent with this hypothesis, the average total number of mutations in those uterine and colon cancers with *DLC1* mutations was significantly higher than in those with wild type *DLC1* (Figure 1B and C).

Somatic mutation of Rho-GAP genes occurs frequently in cancer

To extend the bioinformatic analysis to other Rho-GAPs, we used the TCGA database for the same 12 tumor types for which the three *DLC* genes had been evaluated, to compare the mutation rates for seven other Rho-GAPs that, based on their reported ability to bind RhoA-GTP and their association with cancer, presumptively regulate RhoA-GTP (Table 2A and B). The Rho-GAPs are *ARHGAP35* (also known as p190A Rho-GAP (21,24)), *ARHGAP5* (also known as p190B Rho-GAP (24)), *ARHGAP6* (25), *ARHGAP18* (26,27), *ARHGAP21* (28), *ARHGAP26* (also known as GRAF1 (29,30)) and *ARHGAP28* (31). As with Table 1A and B, the tumor types have been arranged in descending order, from top to bottom, according to the mean number of codon mutations of any type, with Table 2A listing the percentage of codon mutations of any type for the respective Rho-GAP, and Table 2B listing the percentage of missense mutations for these genes.

Compared with the number of tumors with *DLC1* mutations, the percentage of uterine tumors with codon mutations of any kind or with missense mutations was even higher for three of the seven Rho-GAPs: *ARHGAP35* (18.87% any type, 9.81% missense), *ARHGAP5* (9.81% any type, 7.74% missense), and *ARHGAP21* (12.64% any type, 10.38% missense) vs. *DLC1* (9.06% any type, 7.74% missense). However, the mutation rate in the other 11 tumor types for these three Rho-GAPs was lower than for *DLC1* in most instances, although it was similar in a few. The mutation rates of the four other Rho-GAPs were uniformly lower than for *DLC1* in all 12 tumor types. As had been true for the *DLC* genes, at least two-thirds of the mutations in the other Rho-GAPs were missense in most instances. However, the percentage of missense mutations was substantially lower in a few situations,

such as *ARHGAP5* in stomach cancer, where 32% of the mutations were missense, and *ARHGAP35* in uterine cancer, where 52% were missense. We also compared the frequency of missense, nonsense, and frame-shift mutations in the 10 Rho-GAPs, which showed that the frequency of missense mutations was higher than that of nonsense or frame-shift mutations (Supplementary Table S2). Thus, the tumors have selected for missense mutations more frequently than for nonsense or frame-shift mutations.

The most striking observation was seen when the total percentage of tumors with Rho-GAP mutations, including those from the *DLC* genes, was determined (the column labeled Total in Table 2A and B). For uterine cancer and melanoma, at least 28% of the tumors had one or more Rho-GAP mutation of any kind, and more than 25% of these two tumor types had at least one missense mutation of a Rho-GAP gene. For colon, stomach, lung AD, and lung SC, 21–25% of the tumors had mutations of any type, and 17–20% of the tumors had missense mutations. Rectal and esophageal cancer were somewhat lower, but their percentage of tumors with missense mutations was still relatively high, at 13.14% and 16.30%, respectively. By contrast, the percentage of tumors with missense mutations was lower than 6% for the four tumor types with the lowest average number of total mutations: pancreas, liver, breast, and prostate. Esophageal cancer had the highest Rho-GAP mutation rate relative to its total average number of mutations per tumor.

We examined whether a subset of the tumors with Rho-GAP mutations also had a mutation of *RHOA* or *RHOC* (*RHOB* is usually down-regulated in tumors (1)), or whether mutation of a Rho-GAP with mutant Rho did not co-occur. The analysis indicated that Rho-GAP gene mutation and *RHOA* or *RHOC* mutation co-occurred relatively frequently, 6–12% of the time (median 8%; Supplementary Table S3). To place this finding in a more familiar context, we also evaluated whether there was co-occurrence between mutant *NF1* and mutant *KRAS*. Their co-occurrence was found to be even higher, 17%, than for the Rho-GAPs and *RHOA* or *RHOC* (Supplementary Figure S2A and B). Although the vast majority of *NF1* mutations in the database only occurred once, some of the *NF1* mutations arose more than once. These recurrent *NF1* mutations co-occurred with mutant *KRAS* and also occurred in the absence of *KRAS* mutation (Supplementary Figure S2C).

Bioinformatic analysis of *DLC1* missense mutants

For the experimental part of our analysis, we focused on *DLC1*, which had the highest mutation rate among the Rho-GAPs for most tumor types. The *DLC1* missense mutations in the COSMIC database (the TCGA harmonized dataset and Catalogue Of Somatic Mutations In Cancer dataset [Cosmic v74, 2015]) were distributed along its coding sequences (Supplementary Figure S3). Although there are several normal variant *DLC1* mRNAs (32), we focused on mutations that affected variant 2, which is the most highly expressed variant in normal tissue and is by far the variant that has been studied in greatest detail. Variant 2 encodes a 1091 amino acid protein whose SAM (Sterile Alpha Motif) domain lies at its N-terminus and its START (StAR-related lipid-transfer) domain at its C-terminus (Supplementary Figure S3). The Linker Region (LR), which is located downstream from the SAM domain, is the site of several post-translational modifications that can regulate the activity of the protein (16,33,34); this region is required for the protein to localize to

focal adhesions, which has led to a subset of these sequences sometimes being designated the focal adhesion targeting (FAT) region (12). It should also be noted that some mutations in the COSMIC database were localized to sequences that are specific to variant 1, whose encoded protein contains a unique 450 amino acid N-terminal segment that is linked to amino acids 14–1091 of variant 2 protein.

Most Rho-GAP domain point mutants are deficient for Rho-GAP activity and are impaired biologically

Our working hypothesis was that most *DLC1* missense mutations would lead to a DLC1 mutant protein with decreased function compared with wild type DLC1. However, the degree to which these putative decreases could be successfully tested in cells and whether their mechanisms could be elucidated was uncertain. We constructed and analyzed 11 *DLC1* missense mutants, most of which were identified in colorectal cancer in the COSMIC database (v74, 2015) and confirmed by direct reading of the bam file sequences (Supplementary Table S4). Nine of the mutations lie in the Rho-GAP domain, as very few cancer-associated mutants in this domain have been analyzed until now. In addition, we constructed a cancer-associated mutant whose lesion is in the LR, and another whose lesion is in the START domain.

For the DLC1 Rho-GAP domain mutants, we examined 7 identified in colon cancer, one that arose in lung AD, and one in gastric cancer (Supplementary Table S4). To study the mutants, we constructed isogenic GFP-tagged versions of full-length *DLC1* and used wild type *DLC1* as the positive control and either of two “GAP-dead” mutants (DLC1-R677E and DLC1-R718A) as negative controls. Cellular RhoA-GTP levels were determined by transfection of plasmids encoding the full-length versions of 8 of the mutants (all except D671E) into the HCT 116 cell line (Figure 2A), which is a human colon cancer line that does not express detectable *DLC1* mRNA (Supplementary Figure S4). The RhoA-GTP levels for 7 of the mutants (R684Q, D711N, T726M, S730L, R761Q, V790M, and A837G) were high, similar to those of the “GAP-dead” mutant (R718A); those of the mutants with the most conservative change (D758E or D671E) were similar to wild type DLC1.

To verify that the Rho-GAP domain was sufficient to reproduce the RhoA-GTP phenotypes that had been determined with the full-length gene, we made GFP-tagged constructs of the isolated Rho-GAP domain (amino acids 609–878) for most of the mutants examined for full-length DLC1 (Figure 2B). The mutants were transfected into the H1299 cell line, which is a human non-small cell lung cancer line that expresses detectable DLC1 protein (19). The results with the Rho-GAP domain recapitulated those with the full-length gene; those Rho-GAP domain mutants whose high RhoA-GTP was similar to that of the “GAP-dead” mutant (R677E) had also displayed high RhoA-GTP in the full-length constructs, while the low RhoA-GTP of the D758E mutant was similar to the wild type positive control. Furthermore, the RhoA-GTP of the D671E mutant was similar to the wild type.

We also verified that the RhoA-GTP level of the mutants in the Rho-GAP domain constructs correlated with a biomarker for a biochemical signal that lies downstream of Rho-GTP, namely cofilin activity, which depends on Rho-GTP and Cdc42-GTP (35). Mutants in the Rho-GAP construct were transfected into a colon cancer cell line (SW620) that lacks

endogenous DLC1 (Supplementary Figure S4), and phosphorylation of Cofilin Serine-3 was used to assess Cofilin activity (Figure 2C). The results indicated that the two D to E mutants reduced cofilin phosphorylation similarly to wild type DLC1, while the other mutants tested behaved similarly to the two "GAP-dead" mutants (R677E and R718A). All full-length mutants were also analyzed by microscopy for their ability to reduce focal adhesions, a phenomenon that is characteristic of cells with low RhoA-GTP and is seen in cells expressing wild type DLC1, but not those with "GAP-dead" DLC1 (16). This parameter was also found to follow the RhoA-GTP levels seen with the mutants; the two D to E mutants behaved as wild type, while the seven mutants associated with high RhoA-GTP were similar to the "GAP-dead" control mutant (Supplementary Figure S5).

We also tested the full-length mutants for the biological parameter cell migration, which is reduced by wild type DLC1. To study the effect of the full-length mutants on cell migration, transient transfectants of all 9 mutants were made in H1299 cells (Figure 3A and Supplementary Figure S6A). As with their RhoA-GTP levels, the mutants that had displayed high RhoA-GTP were less efficient than wild type in reducing cell migration, while the phenotype of the two D to E mutants, which had wild type Rho-GAP activity, were similar to the wild type. The DLC1 mutants were stably transfected into SW620 cells and then analyzed for their ability to negatively regulate CDC42-GTP, as the Rho-GAP domain of DLC1 possesses the latter biochemical activity, although it is less efficient than that against Rho-GTP (36,37). The mutants that were deficient for reducing RhoA-GTP were also deficient for reducing CDC42-GTP, while the D671E mutant behaved as the wild type (Supplementary Figure S6B). The ability of the stable SW620 transfectants to suppress anchorage-independent growth was also impaired for the same mutants with high RhoA-GTP and high CDC42-GTP (Figure 3B and Supplementary Figure S6B).

An LR mutant and a START domain mutant are deficient for 14-3-3 binding and Caveolin-1 binding, respectively, and are impaired biologically

We examined two other cancer-associated mutants: an S327R mutation in the linker region that arose in a stomach cancer and an E966K mutation in the START domain that arose in a colon cancer. The point mutation in the LR affects a Serine (S327) that was previously found to be involved in the phosphorylation-dependent binding of DLC1 to 14-3-3 adapter/chaperone proteins, which interact with phophoserine- and phosphothreonine-containing motifs (38). With the exception of 14-3-3 sigma, whose expression is restricted to epithelial cells, the human 14-3-3 family members are expressed ubiquitously (39). To determine if the binding of S327R mutant to 14-3-3 differed from that of wild type DLC1, we tested the binding of the DLC1 mutant protein to the proteins encoded by any of three different *14-3-3* genes, namely 14-3-3 beta, 14-3-3 eta, and 14-3-3 theta, by co-transfecting a plasmid encoding the GFP-tagged S327R protein with a plasmid encoding a GST-tagged version of one of the 14-3-3 genes into HEK 293T cells. The GST pull-downs indicated the S327R mutant was deficient for binding all three 14-3-3 proteins (Figure 4A), although it retained some binding to 14-3-3 eta, albeit with reduced efficiency compared to DLC1 wild-type.

The above 14-3-3 binding results differed from those reported by Scholz et al. for a less divergent S327 mutant that they had constructed and studied, S327A. They also identified

a second 14-3-3 binding motif in the LR that involves the phosphorylation of S431. From their experimental analysis of the S327A and S431A single mutants and the S327A/S431A double mutant, they concluded that the S-to-A single mutants bound 14-3-3 similarly to wild type and retained wild type DLC1 activity, while the S-to-A double mutant was deficient. To compare the 14-3-3 binding of the mutants they studied with S327R, we constructed the same single and double mutants as Scholz et al. and, in addition, the S327R/S431A double mutant, and tested the binding ability of these mutants to 14-3-3 theta, the family member that had resulted in the greatest decrease in binding to the DLC1 S327R mutant compared to wild-type (Figure 4A). Consistent with the results of Scholz et al., we found the S327A and S431A single mutants bound 14-3-3 theta similarly to wild type, while the S327A/S431A double mutant bound less efficiently (Figure 4B). In the same experiment, the cancer-associated S327R mutant was deficient for 14-3-3 theta binding, and the S327R/S431A double mutant was even more deficient than the S327A/S431A mutant (Figure 4B).

The cancer-associated E966K point mutation in the START domain lies just downstream from a segment in the START domain that, through analysis of an experimentally constructed DLC1 deletion mutant that lacked amino acids 929–957, we previously identified as being required for efficient binding of DLC1 to caveolin-1 (17,39). To evaluate the binding of the E966K mutant to caveolin-1, we constructed a plasmid encoding a GFP-tagged version of the mutant, which was co-transfected with a plasmid encoding a GST-tagged version of caveolin-1 into HEK 293T cells (Figure 4C). The GST pull-down assay indicated that the E966K mutant had reduced caveolin-1 binding, compared with wild type DLC1, and that the 929–957 deletion mutant was even more deficient for caveolin-1 binding.

We analyzed the S327R and E966K mutants for their ability to reduce Rho-GTP in cells, reduce cell migration, and reduce growth in agar (Figure 5). When transfected into HCT 116 or H1299 cells, both mutants reduced RhoA-GTP similarly to that of the wild type (Figure 5A–C). However, both were as deficient as the “GAP-dead” mutant (R718A) in reducing cell migration in H1299 (Figure 5D). Their ability to reduce growth in agar in SW620 cells was also impaired, although not to the same degree as the “GAP-dead” mutant (Figure 5E).

Discussion

This study has made the unexpected observation that missense and other codon-associated mutations of Rho-GAPs occur frequently in many, but not all, cancer types, and has determined that a variety of mechanisms that lead to decreased function, compared with wild type DLC1, can be found in cancer-associated DLC1 mutants.

When only missense mutations that involve *DLC1–3* were considered for the 12 cancer types evaluated, more than 10% of the tumors in five of these cancer types - uterine, melanoma, colon, stomach, and lung squamous cell - were found to have missense mutations that affected at least one DLC gene, this type of mutation was present in 5–10% of three of the other cancer types – rectum, lung adenocarcinoma, and esophagus - while it was found in fewer than 3% of the other four cancer types. Expanding the mutant analysis to seven additional established or likely Rho-GAPs indicated that cancer-associated missense

mutations of Rho-GAPs are very common. When the ten Rho-GAPs were considered together, missense mutations occurred in 20–26% of four of the twelve cancer types and in 13–19% of four additional tumor types, while they were found in fewer than 7% of the remaining tumor types. These results differ considerably from what was seen for *RHOA* mutations, which were relatively high in stomach cancer, but not in other cancer types. In fact, the frequency of Rho-GAP mutation was lower in stomach cancer than in four of the other tumor types.

The frequency of Rho-GAP mutations tended to parallel the average total number of mutations in each tumor type, but there was considerable variation. The highest number of missense mutations in Rho-GAPs occurred in the two cancer types with the highest number of total mutations, uterine cancer and melanoma. However, while the average total number of mutations in these two cancers differed almost two-fold, being 955 for uterine cancer vs. 495 for melanoma, their frequency of Rho-GAP missense mutations was almost identical, 25.85% vs. 26.34%, respectively. Lung adenocarcinoma, lung squamous cell cancer, and esophageal cancer had an even higher frequency of missense Rho-GAP mutations, relative to their average number total mutations, which was 254, 250, and 133, respectively, while their percentage of tumors with Rho-GAP missense mutations was 17.11%, 20.33%, and 16.30%, respectively. These results suggest that cancer-associated Rho-GAP mutations may be especially important in the above tumor types.

Missense mutations occurred more frequently with *DLC1* than with any other Rho-GAP gene for most of the 12 cancer types. Uterine cancer was a notable exception, as the mutation frequency of ARHGAP35 (9.81%) and ARHGAP21 (10.38%) was higher than for DLC1 (7.74%), which was identical to that of ARHGAP5 (7.74%). Although mutation of the other Rho-GAPs was less frequent, together they made a substantial contribution to the high overall percentage of Rho-GAP mutations in the various tumor types.

We did not unambiguously determine whether the Rho-GAP mutations identified only by bioinformatics were biologically significant, although it is clear that they have been selected for in the tumors where they have arisen. Most of the *DLC1* mutant alleles were heterozygous in the tumors, but some were homozygous, and the mutant *DLC1* and other Rho-GAP alleles co-occurred in 8% of the tumors. Analogous observations were made for comparisons between mutant *NF1* alleles – which are usually considered to be biologically relevant (20) - and mutant *KRAS* in the same tumor database. While mice that have one wild type *DLC1* allele and one null allele develop normally (40), experimental tumorigenicity studies support the biological relevance of a heterozygous loss-of-function mutant *DLC1* allele, as mice carrying one wild type *DLC1* allele and one gene-trapped *DLC1* allele that is null for variant 2, when mated to mice carrying a conditional mutant KRas allele, have an increased incidence of thymic tumors and metastases, and a shortened lifespan (41). More research is needed to firmly establish the biological relevance of heterozygous mutant Rho-GAP alleles in human tumors.

To evaluate the biological relevance of a subset of the *DLC1* missense mutants, we experimentally evaluated a series of cancer-associated *DLC1* mutants, most of which had arisen in colon cancers. Our assessment of *DLC1* mutants with lesions in the Rho-GAP

domain indicated that our cell-based analyses were able to identify a non-wild type phenotype for seven of the nine mutants found in colon cancer, and for two additional mutants identified in other tumor types. The phenotype of the deficient mutants was similar to that of two widely used “GAP-dead” *DLC1* mutants that are deficient for hydrolysis of Rho-GTP to Rho-GDP and for inhibition of cell migration and growth in agar. These mutants displayed a loss-of-function phenotype that was associated with increased Rho-dependent activities and was similar whether the cells with the mutants contained or lacked endogenous *DLC1*. These results strongly imply that the increased Rho activity observed with these mutants is relevant to their selection in the tumors. This interpretation is also consistent with the observation that some tumors had frame-shift mutations in the various Rho-GAP genes, in addition to the tumors that harbored missense mutations. The two mutants in the Rho-GAP domain that displayed phenotypes similar to wild type were those with the most conservative changes, D671E and D758E. It remains possible that these mutants may have an in vivo phenotype that differs from wild type, although the cell-based assays did not clearly identify one.

We also evaluated a missense mutant with a lesion in the LR and another whose lesion was in the START domain. As with most of the mutants with lesions in the Rho-GAP domain, these two mutants were less active biologically than wild type DLC1. However, this phenotype was achieved by a mechanism that is independent of the Rho-GAP activity of DLC1, in contrast to the Rho-GAP domain mutants.

The cancer-associated S327R mutant eliminates a phosphoserine site involved in the interaction of DLC1 with 14-3-3 proteins. An experimental mutant with a lesion at this residue, S327A, was previously found to have wild type DLC1 activity (38), but the cancer-associated mutant, which has a more drastic S-to-R amino acid change, was deficient for binding 14-3-3, for inhibition of cell migration, and for suppression of growth in agar, although it had wild type Rho-GAP activity. In apparent contrast to our results, Sholz et al reported that a DLC1 double mutant (S327/431A) deficient for 14-3-3 protein binding was more active than the wild type for inhibiting cell growth (38). One possibility for this discrepancy is that introduction of the positively charged arginine residue in the S327R mutant could alter the conformation of the protein and interfere with other intra- and intermolecular interactions. Alternatively, differences in cells and/or the experimental system may also account for this divergence.

The START domain mutation, E966K, lies just downstream from a segment in which an experimental deletion mutant that was missing residues 929–957 was previously found to be deficient for several functions associated with wild type DLC1, including caveolin binding, inhibition of cell migration, and inhibition of growth in agar, although its Rho-GAP activity was similar to that of the wild type (17). We found the phenotype of E966K mutant was similar to that of the deletion mutant.

The S327R and E966K mutants represent two alternative GAP-independent mechanisms of DLC1 function, by affecting DLC1 scaffolding functions (its binding to 14-3-3 proteins or Caveolin-1, respectively) without affecting DLC1 Rho-GAP activity. Previous work from several laboratories have described several scaffolding functions of DLC1 that contribute

to its tumor suppressor activities in a Rho-GAP independent manner (reviewed in (42)), including interactions between DLC1 and tensins, talin, and FAK (15,19,43,44), in addition to those between DLC1 and 14-3-3 and Caveolin-1.

In a previous study, Park et al. reported a decrease in the half-life of three cancer-associated DLC1 proteins encoded by mutants associated with gastric cancer as a mechanism for the decreased DLC1 function that they observed (11). They used the DLC1 variant 1 to study their DLC1 mutants, and the protein levels encoded by this variant are much lower than those encoded by variant 2, which is the variant used here to analyze the mutants. In the DLC1 mutants studied here, which are different from those reported by Park et al., we did not observe a major difference in their encoded protein levels compared with the wild type.

Most previous studies of DLC1 in cancer have emphasized changes at the nucleic acid level, such as gene deletion, methylation, and mRNA expression. In addition, Kim et al. found that the Cullin-4A ubiquitin ligase system was active in at least one cancer cell line, leading to ubiquitin-mediated proteasome-dependent degradation of DLC1 protein (45). Here, the Rho-GAP domain mutants highlight the importance of Rho-GAP activity to the biological function of DLC1, while the LR and START domain mutants emphasize the importance of scaffold functions of DLC1 to its biological activity. Analysis of these mutants indicates that DLC1 encodes a multifunctional protein whose biological activity can be reduced by a variety of mechanisms that are relevant to and are selected for in cancer.

Supplementary Material

Refer to Web version on PubMed Central for supplementary material.

Acknowledgements

We thank the National Cancer Institute Center CCR Cancer Research Imaging Core Facilityfor confocal microscopy and Genomic Core Facility for DNA sequencing service, and Drs. Michael DiPrima and Giovanna Tosato from NCI for HT-29, HCT 116, COLO 205, SW620, RKO and MCF-7 cell lines.

Grant Support

This research was supported by the Intramural Research Program, NIH, National Cancer Institute, and Center for Cancer Research.

References

1. Orgaz JL, Herraiz C, Sanz-Moreno V. Rho GTPases modulate malignant transformation of tumor cells. Small GTPases2014;5:e29019 [PubMed: 25036871]
2. Lin Y, Zheng Y. Approaches of targeting Rho GTPases in cancer drug discovery. Expert Opin Drug Discov2015;10:991–1010 [PubMed: 26087073]
3. Kataoka K, Ogawa S. Variegated RHOA mutations in human cancers. Exp Hematol2016;44:1123–9 [PubMed: 27693615]
4. Kakiuchi M, Nishizawa T, Ueda H, Gotoh K, Tanaka A, Hayashi A, et al.Recurrent gain-of-function mutations of RHOA in diffuse-type gastric carcinoma. Nat Genet2014;46:583–7 [PubMed: 24816255]
5. Vigil D, Cherfils J, Rossman KL, Der CJ. Ras superfamily GEFs and GAPs: validated and tractable targets for cancer therapy?Nat Rev Cancer2010;10:842–57 [PubMed: 21102635]

6. Hodge RG, Ridley AJ. Regulating Rho GTPases and their regulators. Nat Rev Mol Cell Biol2016;17:496–510 [PubMed: 27301673]
7. Durkin ME, Yuan BZ, Zhou X, Zimonjic DB, Lowy DR, Thorgeirsson SS, et al.DLC-1:a Rho GTPase-activating protein and tumour suppressor. J Cell Mol Med2007;11:1185–207 [PubMed: 17979893]
8. Lukasik D, Wilczek E, Wasiutynski A, Gornicka B. Deleted in liver cancer protein family in human malignancies (Review). Oncol Lett2011;2:763–8 [PubMed: 22866123]
9. Wang D, Qian X, Rajaram M, Durkin ME, Lowy DR. DLC1 is the principal biologically-relevant down-regulated DLC family member in several cancers. Oncotarget2016;7:45144–57 [PubMed: 27174913]
10. Popescu NC, Goodison S. Deleted in liver cancer-1 (DLC1): an emerging metastasis suppressor gene. Mol Diagn Ther2014;18:293–302 [PubMed: 24519699]
11. Park H, Cho SY, Kim H, Na D, Han JY, Chae J, et al.Genomic alterations in BCL2L1 and DLC1 contribute to drug sensitivity in gastric cancer. Proc Natl Acad Sci U S A2015;112:12492–7 [PubMed: 26401016]
12. Liao YC, Shih YP, Lo SH. Mutations in the focal adhesion targeting region of deleted in liver cancer-1 attenuate their expression and function. Cancer Res2008;68:7718–22 [PubMed: 18829524]
13. Ravi A, Kaushik S, Ravichandran A, Pan CQ, Low BC. Epidermal growth factor activates the Rho GTPase-activating protein (GAP) Deleted in Liver Cancer 1 via focal adhesion kinase and protein phosphatase 2A. J Biol Chem2015;290:4149–62 [PubMed: 25525271]
14. Forbes S, Clements J, Dawson E, Bamford S, Webb T, Dogan A, et al.Cosmic 2005. British journal of cancer2006;94:318–22 [PubMed: 16421597]
15. Qian X, Li G, Asmussen HK, Asnaghi L, Vass WC, Braverman R, et al.Oncogenic inhibition by a deleted in liver cancer gene requires cooperation between tensin binding and Rho-specific GTPase-activating protein activities. Proc Natl Acad Sci U S A2007;104:9012–7 [PubMed: 17517630]
16. Tripathi BK, Grant T, Qian X, Zhou M, Mertins P, Wang D, et al.Receptor tyrosine kinase activation of RhoA is mediated by AKT phosphorylation of DLC1. J Cell Biol2017;in press
17. Du X, Qian X, Papageorge A, Schetter AJ, Vass WC, Liu X, et al.Functional interaction of tumor suppressor DLC1 and caveolin-1 in cancer cells. Cancer Res2012;72:4405–16 [PubMed: 22693251]
18. Qian X, Li G, Vass WC, Papageorge A, Walker RC, Asnaghi L, et al.The Tensin-3 protein, including its SH2 domain, is phosphorylated by Src and contributes to tumorigenesis and metastasis. Cancer Cell2009;16:246–58 [PubMed: 19732724]
19. Li G, Du X, Vass WC, Papageorge AG, Lowy DR, Qian X. Full activity of the deleted in liver cancer 1 (DLC1) tumor suppressor depends on an LD-like motif that binds talin and focal adhesion kinase (FAK). Proc Natl Acad Sci U S A2011;108:17129–34 [PubMed: 21969587]
20. Philpott C, Tovell H, Frayling IM, Cooper DN, Upadhyaya M. The NF1 somatic mutational landscape in sporadic human cancers. Hum Genomics2017;11:13 [PubMed: 28637487]
21. Lawrence MS, Stojanov P, Mermel CH, Robinson JT, Garraway LA, Golub TR, et al.Discovery and saturation analysis of cancer genes across 21 tumour types. Nature2014;505:495–501 [PubMed: 24390350]
22. Liu D, Keijzers G, Rasmussen LJ. DNA mismatch repair and its many roles in eukaryotic cells. Mutat Res2017;773:174–87
23. Baretti M, Le DT. DNA mismatch repair in cancer. Pharmacol Ther2018;189:45–62 [PubMed: 29669262]
24. Frank SR, Kollmann CP, Luong P, Galli GG, Zou L, Bernards A, et al.p190 RhoGAP promotes contact inhibition in epithelial cells by repressing YAP activity. J Cell Biol2018;217:3183–201 [PubMed: 29934311]
25. Tanaka A, Ishikawa S, Ushiku T, Yamazawa S, Katoh H, Hayashi A, et al.Frequent CLDN18-ARHGAP fusion in highly metastatic diffuse-type gastric cancer with relatively early onset. Oncotarget2018;9:29336–50 [PubMed: 30034621]

26. Maeda M, Hasegawa H, Hyodo T, Ito S, Asano E, Yuang H, et al.ARHGAP18, a GTPase-activating protein for RhoA, controls cell shape, spreading, and motility. Mol Biol Cell2011;22:3840–52 [PubMed: 21865595]
27. Li Y, Ji S, Fu L, Jiang T, Wu D, Meng F. Over-expression of ARHGAP18 suppressed cell proliferation, migration, invasion, and tumor growth in gastric cancer by restraining over-activation of MAPK signaling pathways. Onco Targets Ther2018;11:279–90 [PubMed: 29386906]
28. Rosa LRO, Soares GM, Silveira LR, Boschero AC, Barbosa-Sampaio HCL. ARHGAP21 as a master regulator of multiple cellular processes. J Cell Physiol2018;233:8477–81 [PubMed: 29856495]
29. Qian Z, Qian J, Lin J, Yao DM, Chen Q, Ji RB, et al.GTPase regulator associated with the focal adhesion kinase (GRAF) transcript was down-regulated in patients with myeloid malignancies. J Exp Clin Cancer Res2010;29:111 [PubMed: 20704716]
30. Yao F, Kausalya JP, Sia YY, Teo AS, Lee WH, Ong AG, et al.Recurrent Fusion Genes in Gastric Cancer: CLDN18-ARHGAP26 Induces Loss of Epithelial Integrity. Cell Rep2015;12:272–85 [PubMed: 26146084]
31. Kasuya K, Nagakawa Y, Hosokawa Y, Sahara Y, Takishita C, Nakajima T, et al.RhoA activity increases due to hypermethylation of ARHGAP28 in a highly liver-metastatic colon cancer cell line. Biomed Rep2016;4:335–9 [PubMed: 26998271]
32. Ko FC, Yeung YS, Wong CM, Chan LK, Poon RT, Ng IO, et al.Deleted in liver cancer 1 isoforms are distinctly expressed in human tissues, functionally different and under differential transcriptional regulation in hepatocellular carcinoma. Liver Int2010;30:139–48 [PubMed: 19874489]
33. Ko FC, Ping Yam JW. Regulation of deleted in liver cancer 1 tumor suppressor by protein-protein interactions and phosphorylation. International journal of cancer Journal international du cancer2014;135:264–9 [PubMed: 24114040]
34. Tripathi BK, Qian X, Mertins P, Wang D, Papageorge AG, Carr SA, et al.CDK5 is a major regulator of the tumor suppressor DLC1. J Cell Biol2014;207:627–42 [PubMed: 25452387]
35. Kanellos G, Frame MC. Cellular functions of the ADF/cofilin family at a glance. J Cell Sci2016;129:3211–8 [PubMed: 27505888]
36. Healy KD, Hodgson L, Kim TY, Shutes A, Maddileti S, Juliano RL, et al.DLC-1 suppresses non-small cell lung cancer growth and invasion by RhoGAP-dependent and independent mechanisms. Mol Carcinog2008;47:326–37 [PubMed: 17932950]
37. Qian X, Durkin ME, Wang D, Tripathi BK, Olson L, Yang XY, et al.Inactivation of the Dlc1 gene cooperates with downregulation of p15INK4b and p16Ink4a, leading to neoplastic transformation and poor prognosis in human cancer. Cancer Res2012;72:5900–11 [PubMed: 23010077]
38. Scholz RP, Regner J, Theil A, Erlmann P, Holeiter G, Jahne R, et al.DLC1 interacts with 14-3-3 proteins to inhibit RhoGAP activity and block nucleocytoplasmic shuttling. J Cell Sci2009;122:92–102 [PubMed: 19066281]
39. Freeman AK, Morrison DK. 14-3-3 Proteins: diverse functions in cell proliferation and cancer progression. Semin Cell Dev Biol2011;22:681–7 [PubMed: 21884813]
40. Durkin ME, Avner MR, Huh CG, Yuan BZ, Thorgeirsson SS, Popescu NC. DLC-1, a Rho GTPase-activating protein with tumor suppressor function, is essential for embryonic development. FEBS Lett2005;579:1191–6 [PubMed: 15710412]
41. Sabbir MG, Prieditis H, Ravinsky E, Mowat MR. The role of Dlc1 isoform 2 in K-Ras2(G12D) induced thymic cancer. PloS one2012;7:e40302 [PubMed: 22792269]
42. Barras D, Widmann C. GAP-independent functions of DLC1 in metastasis. Cancer Metastasis Rev2014;33:87–100 [PubMed: 24338004]
43. Liao YC, Si L, deVere White RW, Lo SH. The phosphotyrosine-independent interaction of DLC-1 and the SH2 domain of cten regulates focal adhesion localization and growth suppression activity of DLC-1. J Cell Biol2007;176:43–9 [PubMed: 17190795]
44. Zacharchenko T, Qian X, Goult BT, Jethwa D, Almeida TB, Ballestrem C, et al.LD Motif Recognition by Talin: Structure of the Talin-DLC1 Complex. Structure2016;24:1130–41 [PubMed: 27265849]

45. Kim TY, Jackson S, Xiong Y, Whitsett TG, Lobello JR, Weiss GJ, et al.CRL4A-FBXW5-mediated degradation of DLC1 Rho GTPase-activating protein tumor suppressor promotes non-small cell lung cancer cell growth. Proc Natl Acad Sci U S A2013;110:16868–73 [PubMed: 24082123]

Significance:

Findings indicate that point mutation of Rho-GAP genes is unexpectedly frequent in several cancer types, with DLC1 mutants exhibiting reduced function by various mechanisms.

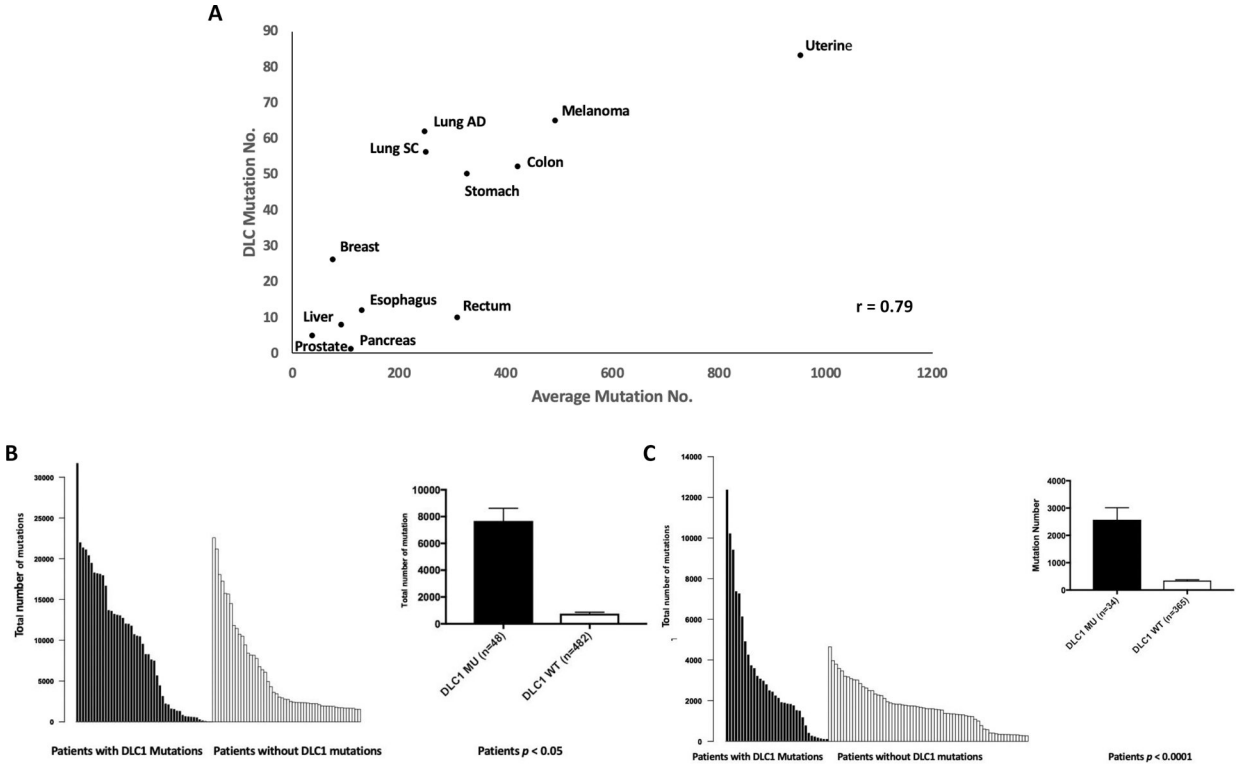

Figure 1. Correlations between the frequency of *DLC1* mutation and total number of mutations in 12 tumor types in TCGA.

(A) Correlation for the 12 tumor types between total number of codon mutations and number of *DLC1* mutations. r = 0.79. **(B)** Uterine cancer: Total number of mutations vs. *DLC1* mutations. The total number of all codon mutations are plotted for individual patients. Left panel: the dark vertical bars represent each of the 48 patients with one or more *DLC1* mutation, while the light vertical bars represent each of the 52 patients with the highest number of total codon mutations who have wild type *DLC1*. Right panel: The Statistical analysis used the Mann-Whitney U test, which compared the total mutation numbers of the patients with and without DLC1 mutations. The vertical axis represents the average value plus standard error. **(C)** Colon cancer: Total number of mutations vs. *DLC1* mutations. The data are presented and analyzed similarly to B, except that the dark vertical bars represent each of the 34 patients with *DLC1* mutations, while the light vertical bars represent each of the 66 patients with the highest number of total codon mutations who have wild type *DLC1*.

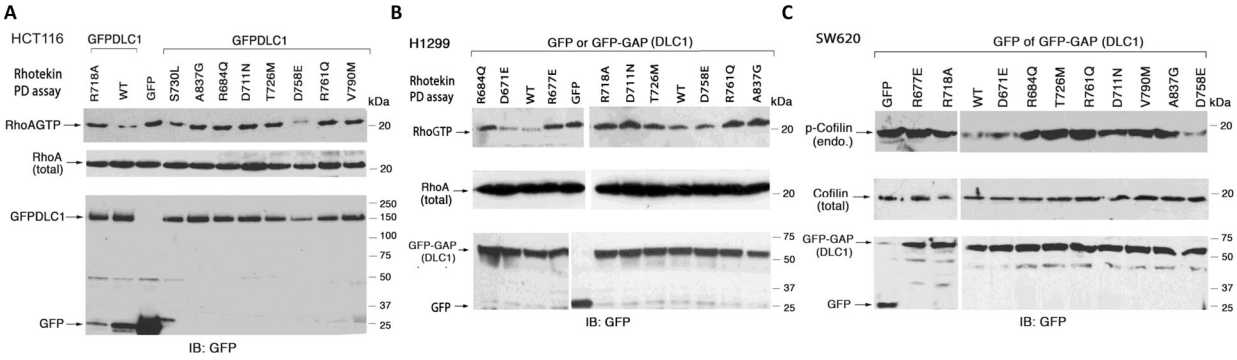

Figure 2. Most DLC1 mutants with missense mutation in the Rho-GAP domain are less active than WT DLC1.

(A) HCT 116 cells were transiently transfected with GFP or full-length GFP-DLC1 followed by Rhotekin pull-down assay to detect their RhoA-GTP levels. The GFP expression level is shown for the transfectants. (**B)** H1299 cells were transiently transfected with GFP or GFP-GAP followed by Rhotekin pull down assay. The expression level of GFP-tagged proteins is shown for the transfectants. (**C)** The phospho-cofilin levels in SW620 cells transiently expressing GFP or GFP-GAP were analyzed by immunoblot. The expression level of GFP, total RHOA, and Cofilin are also shown in each panel.

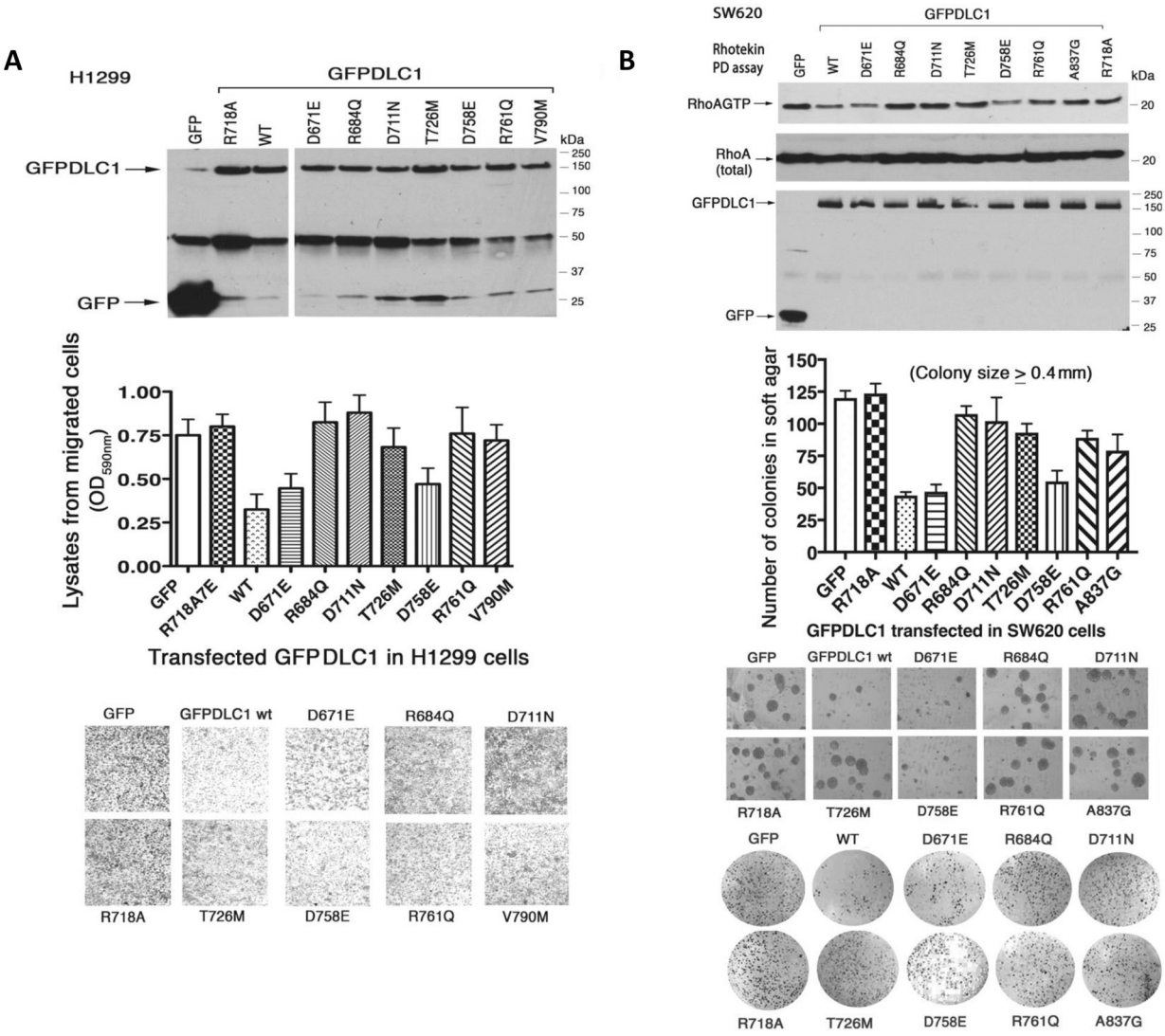

Figure 3. Compared with WT DLC1, biological activity is reduced for most DLC1 mutants with mutations in the Rho-GAP domain.

(A) H1299 cells transiently expressing GFP or GFP-DLC1 (top) were analyzed for cell migration in transwell dishes. Representative micrographs of migrated cells are shown (bottom). The total number of migrated cells, in triplicate, for each mutant is shown as mean ± SD (middle). **(B)** SW620 stable clones expressing GFP or GFP-DLC1 mutants were analyzed by Rhotekin PD assay (top). Cells were seeded in soft agar for 3 weeks. Representative views of colonies under microscope and the stained colonies in the dish are shown (bottom). Number of colonies (≥ 0.4 mm) in triplicate dishes have been plotted as mean ± SD (middle).

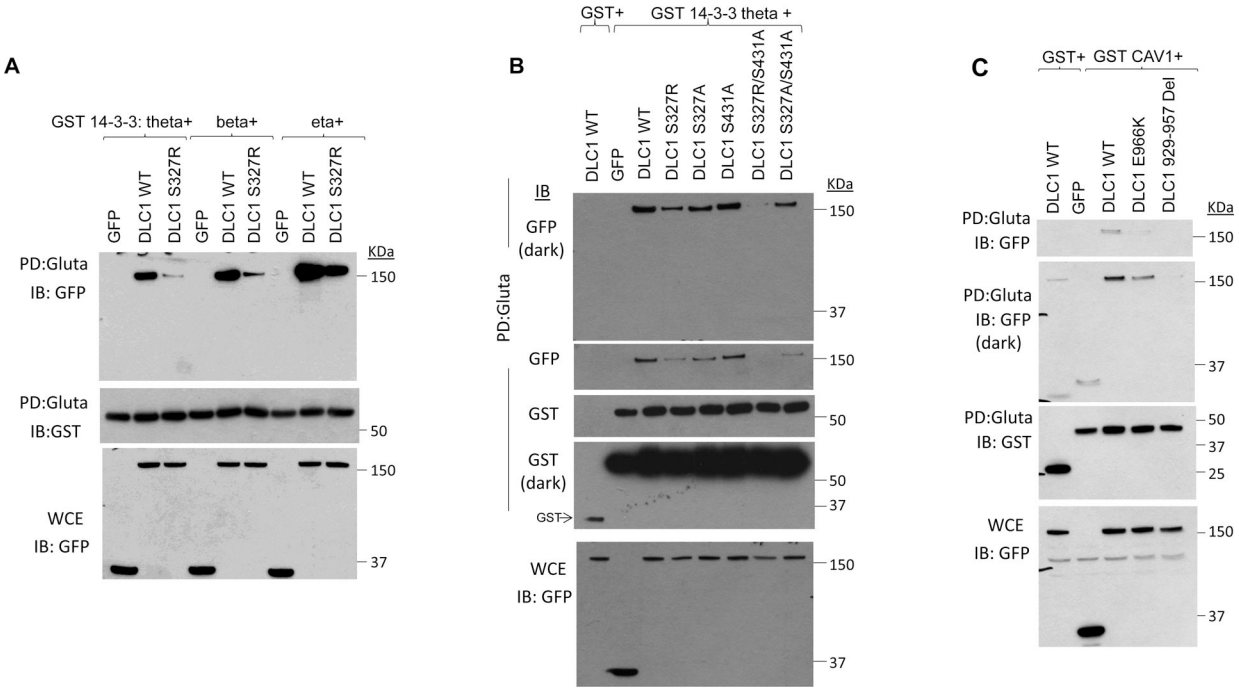

Figure 4. Interaction between DLC1 mutants and GST 14-3-3 proteins or GST Caveolin-1.

(A, B) DLC1 S327R mutant and double mutant S327R/S431A are deficient for binding to GST 14-3-3 proteins. As indicated in the panels, HEK 293T cells were cotransfected with GST or GST 14-3-3 proteins (theta, beta, or eta) and GFP, GFP-DLC1-WT, or GFP-DLC1 mutants. After 48 hours, cells were lysed and pulled-down by Glutathione sepharose-4B (Gluta) and immunoblotted (IB) using GFP or GST antibodies. **(C)** DLC1 E966K mutant binds poorly to GST Caveolin-1 (GST CAV1). HEK 293T cells were cotransfected with GST or GST Caveolin-1 and GFP, GFP-DLC1-WT or GFP-DLC1-E966K mutant and subjected to Glutathione pull-down as described for (A, B). A deletion mutant of DLC1 lacking amino acids 929–957 was used in the pull-down as a negative control for Caveolin-1 binding (see text). WCE: whole cell extracts.

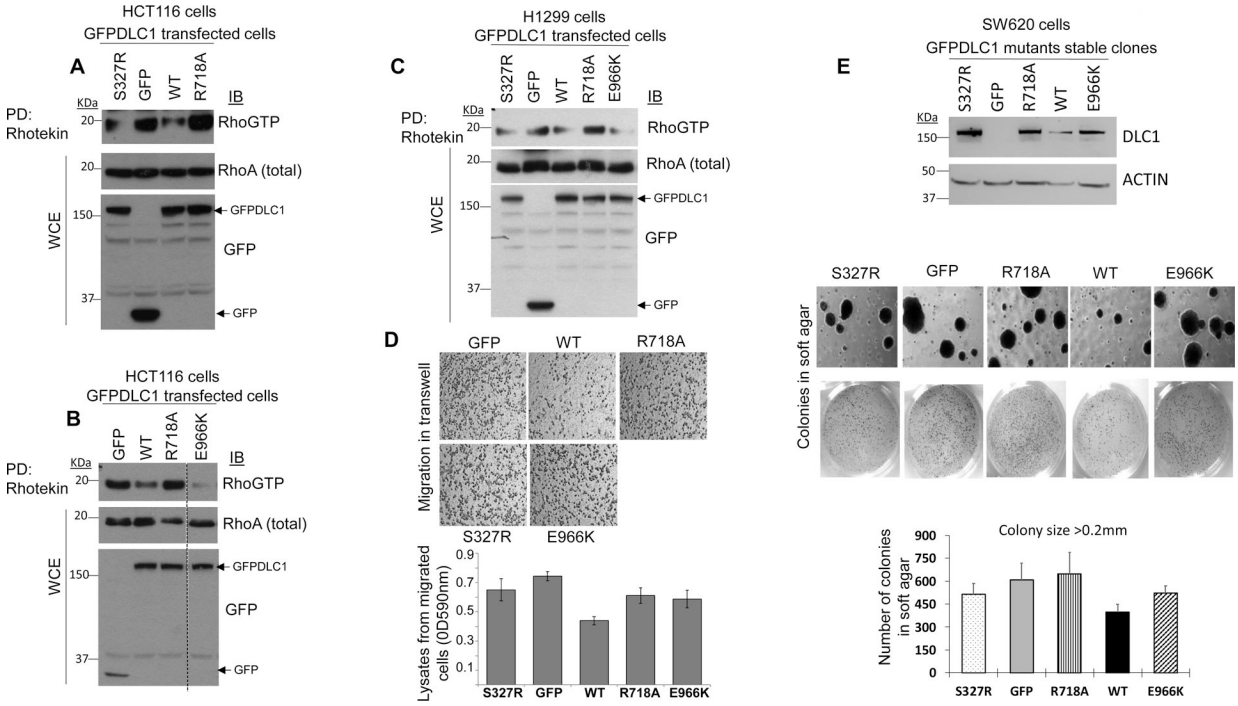

Figure 5. DLC1 S327R and E966K mutants have WT Rho-GAP activity, but inhibit cell migration and colony formation in soft agar less efficiently than DLC1-WT.

(A, B, C) Rho-GAP activity. Active Rho (GTP) in HCT 116 (A, B) or H1299 (C) cells expressing DLC1-WT or the indicated mutants were analyzed by Rhotekin pull-down (PD) assay followed by anti-RHOA immunoblotting (IB). GFP-DLC1 expression and total RHOA expression were also confirmed by immunoblotting. **(D)** Migration in transwell. H1299 cells were transfected with the indicated constructs. 24 hours after transfection, 1×10^5 cells were seeded in a transwell dish and allow to migrate for 18 hours. The migrated cells were stained with crystal violet, photographed (upper panel), and quantified at OD590nm (lower panel). The total number of migrated cells, in triplicate, for each mutant is shown as mean ± SD. **(E)** Soft agar growth. Stable clones for control GFP, GFP-DLC1-WT or the indicated mutants were generated in SW620 cells. 1×10^5 cells were seeded in soft agar and allow to form colonies for approximately 28 days, and those colonies >0.2mm were photographed (middle panel) and counted (lower panel). Number of colonies (≥ 0.2mm) in triplicate dishes have been plotted as mean ± SD. DLC1 expression was confirmed by immunoblotting (upper panel).

Table 1.
DLC1–3 and RHOA mutations in 12 tumor types in TCGA.

The mutants for the 12 tumor types have been identified from the TCGA mutation database in the GDC Data Portal, from which the number of mutants (MU) and the percentage (PCT) of total patients with that tumor type who have the relevant mutations have been calculated. No = the number of tumors of that type. MED MU = median number of mutations for that tumor type. AVE MU = mean number of mutations for that tumor type. **(A)**All codon mutations for each gene. The mutations include missense mutations, nonsense mutations, frame-shift deletions, frame-shift insertions, in-frame deletions, nonstop mutations, in-frame insertions, translation start-site changes, splice-region mutations, and splice-site mutations. **(B)**Missense mutations for each gene.

A

TUMOR	No	MED MU	AVE MU	DLC1		DLC2		DLC3		DLC Total		RhoA	
				MU	PCT	MU	PCT	MU	PCT	MU	PCT	MU	PCT
UTERINE	530	89	955	48	9.06	36	6.79	44	8.30	83	15.66	12	2.26
MELANOMA	467	277	495	32	6.85	29	6.21	13	2.78	65	13.92	6	1.28
COLON	399	112	425	34	8.52	12	3.01	16	4.01	52	13.03	7	1.75
STOMACH	437	109	330	31	7.09	13	2.97	12	2.75	50	11.44	20	4.58
RECTUM	137	95	312	6	4.38	0.00	0.00	4	2.92	10	7.30	1	0.73
LUNG AD	567	169	254	31	5.47	15	2.65	15	2.65	56	9.88	5	0.88
LUNG SC	492	205	250	37	7.52	13	2.64	14	2.85	62	12.60	3	0.61
ESOPHAGUS	184	101	133	6	3.26	5	2.72	1	0.54	12	6.52	3	1.63
PANCREAS	178	34	112	1	0.56	0	0.00	1	0.56	1	0.56	1	0.56
LIVER	364	76	94	4	1.10	2	0.55	2	0.55	8	2.20	0	0.00
BREAST	986	39	78	15	1.52	4	0.41	7	0.71	26	2.64	6	0.61
PROSTATE	495	24	40	2	0.40	2	0.40	2	0.40	5	1.01	2	0.40

B

TUMOR	AVG MU (all codons)	DLC1		DLC2		DLC3		DLC Total		RhoA	
		MU	PCT	MU	PCT	MU	PCT	MU	PCT	MU	PCT
UTERINE	955	41	7.74	33	6.23	34	6.42	70	13.21	10	1.89
MELANOMA	495	26	5.57	27	5.78	12	2.57	56	11.99	5	1.07
COLON	425	28	7.02	11	2.76	12	3.01	43	10.78	5	1.25
STOMACH	330	26	5.95	11	2.52	11	2.52	44	10.07	20	4.58
RECTUM	312	6	4.38	0	0.00	3	2.19	9	6.57	1	0.73
LUNG AD	254	24	4.23	15	2.65	11	1.94	46	8.11	4	0.71
LUNG SC	250	34	6.91	13	2.64	11	2.24	56	11.38	3	0.61
ESOPHAGUS	133	5	2.72	5	2.72	1	0.54	11	5.98	3	1.63
PANCREAS	112	1	0.56	0	0.00	1	0.56	1	0.56	1	0.56
LIVER	94	4	1.10	2	0.55	1	0.27	7	1.92	0	0.00
BREAST	78	12	1.22	2	0.20	7	0.71	21	2.13	5	0.51
PROSTATE	40	1	0.20	1	0.20	2	0.40	4	0.81	2	0.40

Table 2.
Mutants of seven Rho-GAP genes in the 12 tumor types in TCGA.

The mutants were identified from the TCGA mutation database in the GDC Data Portal. **(A)**All codon mutations for each gene. **(B)**Missense mutations for each gene. * Total = total mutations in DLC1–3 and the other 7 Rho-GAPs.

A

TUMOR	AVG MU	ARHGAP35 (P190A)		ARHGAP5 (P190B)		ARHGAP6		ARHGAP18		ARHGAP21		ARHGAP26		ARHGAP28		Total	
		MU	PCT	MU	PCT	MU	PCT	MU	PCT	MU	PCT	MU	PCT	MU	PCT	MU	PCT
UTERINE	**955**	**100**	**18.87**	**52**	**9.81**	**38**	**7.17**	**25**	**4.72**	**67**	**12.64**	**29**	**5.47**	**32**	**6.04**	**185**	**34.91**
MELANOMA	495	19	4.07	19	4.07	21	4.5	11	2.36	28	6.00	21	4.50	15	3.21	133	28.48
COLON	425	23	5.76	23	5.76	12	3.01	9	2.26	27	6.77	7	1.75	20	5.01	99	24.81
STOMACH	330	19	4.35	28	6.41	12	2.75	5	1.14	10	2.29	6	1.37	13	2.97	101	23.11
RECTUM	312	4	2.92	5	3.65	2	1.46	3	2.19	8	5.84	4	2.92	2	1.46	21	15.33
LUNG AD	254	18	3.17	14	2.47	18	3.17	5	0.88	21	3.70	3	0.53	3	0.53	118	20.81
LUNG SC	250	29	5.89	12	2.44	11	2.24	5	1.02	15	3.05	3	0.61	6	1.22	123	25.00
ESOPHAGUS	133	4	2.17	5	2.72	1	0.54	0	0.00	7	3.80	1	0.54	7	3.8	32	17.39
PANCREAS	112	1	0.56	3	1.69	2	1.12	1	0.56	3	1.69	0	0.00	1	0.56	7	3.93
LIVER	94	6	1.65	4	1.10	2	0.55	1	0.27	1	0.27	2	0.55	0	0.00	24	6.59
BREAST	78	15	1.52	10	1.01	4	0.41	5	0.51	13	1.32	8	0.81	7	0.71	72	7.30
PROSTATE	40	2	0.40	4	0.81	1	0.20	1	0.20	4	0.81	1	0.20	1	0.20	14	2.83

B

TUMOR	AVG MU	ARHGAP35 (P190A)		ARHGAP5 (P190B)		ARHGAP6		ARHGAP18		ARHGAP21		ARHGAP26		ARHGAP28		Total	
		MU	PCT	MU	PCT	MU	PCT	MU	PCT	MU	PCT	MU	PCT	MU	PCT	MU	PCT
UTERINE	955	52	9.81	41	7.74	33	6.23	19	3.58	55	10.38	24	4.53	28	5.28	137	25.85
MELANOMA	495	16	3.43	19	4.07	21	4.50	10	2.14	24	5.14	21	4.50	14	3.00	123	26.34
COLON	425	19	4.76	10	2.51	10	2.51	6	1.50	20	5.01	4	1.00	15	3.76	79	19.8
STOMACH	330	14	3.2	9	2.06	9	2.06	2	0.46	8	1.83	4	0.92	11	2.52	79	18.08
RECTUM	312	4	2.92	3	2.19	2	1.46	3	2.19	7	5.11	4	2.92	2	1.46	18	13.14
LUNG AD	254	13	2.29	13	2.29	16	2.82	2	0.35	17	3.00	3	0.53	1	0.18	97	17.11
LUNG SC	250	18	3.66	7	1.42	8	1.63	4	0.81	13	2.64	3	0.61	6	1.22	100	20.33
ESOPHAGUS	133	3	1.63	5	2.72	1	0.54	0	0.00	6	3.26	1	0.54	6	3.26	30	16.30
PANCREAS	112	1	0.56	1	0.56	2	1.12	1	0.56	3	1.69	0	0.00	1	0.56	5	2.81
LIVER	94	5	1.37	3	0.82	2	0.55	1	0.27	1	0.27	0	0.00	0	0.00	19	5.22
BREAST	78	5	0.51	8	0.81	4	0.41	5	0.51	13	1.32	7	0.71	7	0.71	57	5.78
PROSTATE	40	1	0.20	4	0.81	1	0.20	1	0.20	3	0.61	1	0.20	0	0.00	12	2.42